Not All Rollouts are Useful: Down-Sampling Rollouts in LLM Reinforcement Learning

Yixuan Even Xu* *yixuanx@cs.cmu.edu*
Carnegie Mellon University

Yash Savani* *ysavani@cs.cmu.edu*
Carnegie Mellon University

Fei Fang *feif@cs.cmu.edu*
Carnegie Mellon University

J. Zico Kolter *zkolter@cs.cmu.edu*
Carnegie Mellon University

Reviewed on OpenReview: *https://openreview.net/forum?id=MfHOmgqVXM*

Abstract

Reinforcement learning with verifiable rewards (RLVR) has emerged as the leading approach for enhancing reasoning capabilities in large language models. However, it faces a fundamental compute and memory asymmetry: rollout generation is embarrassingly parallel and memory-light, whereas policy updates are communication-heavy and memory-intensive. To address this, we introduce **PODS** (**P**olicy **O**ptimization with **D**own-**S**ampling), which decouples rollout generation from policy updates by training only on a strategically selected subset of rollouts, maintaining learning quality while dramatically reducing update costs. We propose a principled subset selection criterion—*max-variance down-sampling*—that maximizes the variance of reward in the selected subset, and provide an efficient $O(n \log n)$ implementation of this rule. Empirically, Group Relative Policy Optimization (GRPO) coupled with PODS achieves the peak test accuracy of vanilla GRPO at least $\mathbf{1.7}\times$ **faster** across the different reasoning benchmarks and hardware configurations we tested.

1 Introduction

Reinforcement learning with verifiable rewards (RLVR) has driven recent breakthroughs in solving math problems, code generation, and general reasoning for large language models (LLMs) (Jaech et al., 2024; Ziegler et al., 2019; Ouyang et al., 2022; Stiennon et al., 2020). RLVR algorithms such as Proximal Policy Optimization (PPO) (Schulman et al., 2017) and Group Relative Policy Optimization (GRPO) (Shao et al., 2024) share a two-phase structure: an *inference phase*, which generates rollouts given a prompt, and a *policy-update phase*, which updates the model parameters using the rewards calculated on those rollouts.

These two phases place different computational demands on the hardware. Inference is embarrassingly parallel and relatively memory-light, enabling modern accelerators to produce thousands of rollouts concurrently. Although generating a single rollout may have high latency due to autoregressive decoding, batching rollouts amortizes the per-token latency and yields higher throughput. Policy updates, on the other hand, scale poorly with batch size: they are memory- and communication-intensive, requiring full-precision optimizer states and cross-device synchronization of gradients and parameters. This asymmetry creates a fundamental bottleneck: systems must either throttle inference (underutilizing compute) or resort to memory-saving techniques like gradient accumulation (increasing communication overhead and policy update latency), both of which hurt training efficiency. Fig. 1 provides empirical evidence for this computational asymmetry.

*Equal contribution.

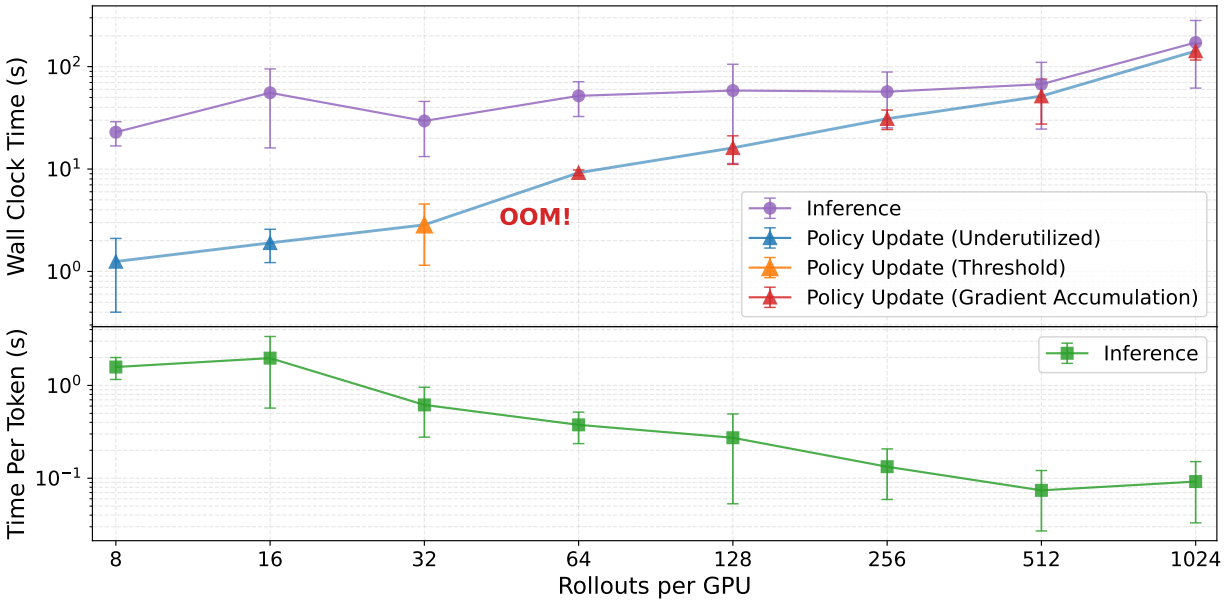

Figure 1: **Inference scales efficiently while policy updates become memory-bound in RLVR.** Empirical timing breakdown when fine-tuning Qwen2.5-3B-Instruct on GSM8K using 8 A100-80GB GPUs with varying rollouts per GPU. **Top:** Total wall-clock time per iteration. Policy updates hit memory limits after 32 rollouts per GPU (Out of memory beyond this point), requiring gradient accumulation that dramatically slows training. **Bottom:** Per-token inference time decreases 21× through batching (from 8 to 512 rollouts), saturating beyond 512. This demonstrates the core asymmetry that PODS exploits: inference parallelizes efficiently while policy updates become memory-bound.

A key observation of our work is: *not all rollouts contribute equally to model improvement.* Beyond a certain scale, additional rollouts provide diminishing returns and can even degrade learning signals through redundant information. This suggests a natural solution: generate large batches of rollouts during the scalable inference phase, but train selectively on only the most informative subset during the policy update phase, avoiding the latency overhead of memory-saving techniques. We formalize this idea in **PODS** (**P**olicy **O**ptimization with **D**own-**S**ampling). As illustrated in Fig. 2, PODS maximizes hardware utilization by generating n rollouts per prompt but updating on only $m < n$ informative samples selected by a principled down-sampling rule.

Within the PODS framework, we introduce *max-variance down-sampling*, a principled criterion that selects the subset of rollouts with the greatest reward variance of the selected subset, thereby preserving strong contrastive signals. We show that the resulting combinatorial problem can be solved in $O(n \log n)$ time and, in the common binary-reward setting, reduces to picking the $m/2$ highest-reward and $m/2$ lowest-reward rollouts. We evaluate PODS with GRPO on GSM8K (Cobbe et al., 2021), MATH (Hendrycks et al., 2021) and the Chemistry subset of SciKnowEval (Feng et al., 2024) across multiple model and hardware configurations, demonstrating that it achieves the peak test accuracy of baseline GRPO at least **1.7× faster**.

2 Related Work

Reinforcement learning for LLM reasoning. Reinforcement learning has emerged as a powerful paradigm for enhancing the reasoning capabilities of LLMs across math, coding, and problem-solving domains (Jaech et al., 2024; Shao et al., 2024; Kazemnejad et al., 2024). Although classical algorithms such as Proximal Policy Optimization (PPO) (Schulman et al., 2017) laid the foundation, recent work has tailored them specifically to language models. Group Relative Policy Optimization (GRPO) (Shao et al., 2024) has gained prominence for reasoning tasks because of its implementation simplicity, competitive performance relative to PPO, and lack of a separate critic network. OpenAI o1 (OpenAI, 2024) and DeepSeek R1 (Guo et al., 2025),

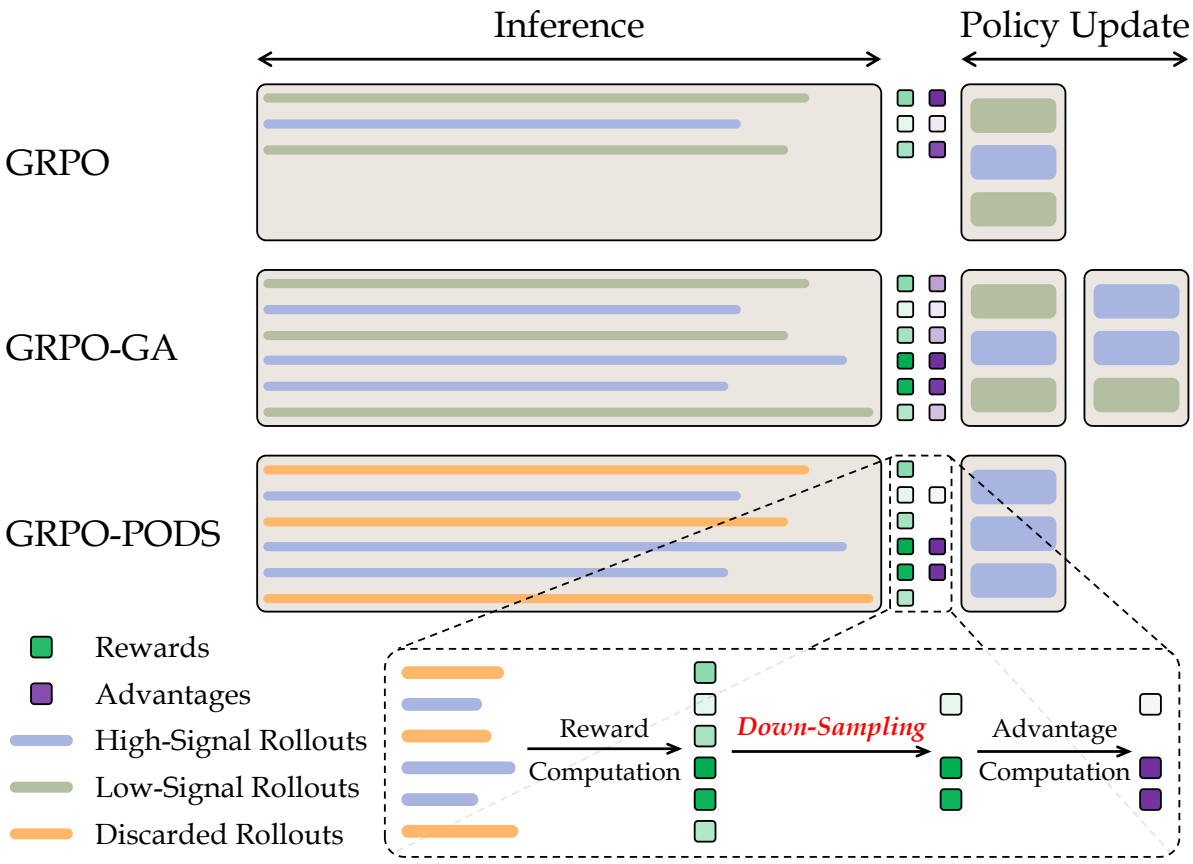

Figure 2: Visualization of three training strategies: vanilla GRPO, GRPO with gradient accumulation (GRPO-GA), and GRPO with PODS (GRPO-PODS). Vanilla GRPO generates n rollouts and trains on all of them, leaving inference hardware underutilized due to the asymmetric computational demands of the two phases. GRPO-GA alleviates this issue with memory-saving techniques such as gradient accumulation, but at the cost of more sequential steps in the policy-update phase. In contrast, GRPO-PODS also generates n rollouts but trains on only m carefully selected examples, maximizing inference utilization, avoiding gradient-accumulation overhead, and providing a cleaner learning signal that yields better final performance.

which used large-scale RL, have sparked interest in reasoning-focused RL methods (Chen et al., 2025; Hu et al., 2025; Hu, 2025; Cui et al., 2025). Meanwhile, value-based approaches like PPO remain central (Yuan et al., 2025a;b), alongside complementary techniques such as Monte Carlo Tree Search (Gao et al., 2024; Xie et al., 2024) and multi-agent methods (FAIR et al., 2022). A recent line of work has also explored data selection for improving RL methods for LLM training. Specifically, prompt selection and filtering has gained significant attention from works such as DAPO (Yu et al., 2025), SRPO (Zhang et al., 2025), Reinforce-Rej (Xiong et al., 2025), Polaris (An et al., 2025), GRESO (Zheng et al., 2025) and VAPO (Yuan et al., 2025a). Our method advances this line of work by focusing on down-sampling rollouts within each prompt, instead of selecting or filtering prompts themselves. By tackling this computational-efficiency bottleneck, our approach complements existing methods and can be combined with them to further improve reasoning performance.

Down-sampling and data selection. The scale of modern machine learning necessitates effective data management strategies, particularly as datasets grow larger, noisier, and more imbalanced. Training on the full dataset can be prohibitively expensive, motivating sophisticated data-selection and down-sampling methods. Such techniques succeed across diverse settings—from theoretical results in clustering (Har-Peled & Mazumdar, 2004), regression (Li et al., 2013; Rudelson & Vershynin, 2007; Clarkson, 2010) to practical systems in speech recognition (Liu et al., 2015; Wei et al., 2014) and computer vision (Kaushal et al., 2019;

Bankes et al., 2024). In reinforcement learning, prioritized experience replay (Schaul et al., 2015) and related methods (Hou et al., 2017; Saglam et al., 2023; Cusumano-Towner et al., 2025) highlight the value of selective sampling from experience buffers. More recently, careful data selection has become central to foundation-model training (Goyal et al., 2024; Schuhmann et al., 2021; Gadre et al., 2023) and emerging applications such as computational advertising (Bei et al., 2023; Gravin et al., 2024). Yet, to our knowledge, we are the first to apply principled down-sampling to the rollout-generation stage of LLM reinforcement learning, mitigating a key computational bottleneck while strengthening the learning signal.

3 Down-Sampling Rollouts in GRPO

In this section, we present our approach to resolving the computational asymmetry between inference and policy updates in LLM reinforcement learning. We first review the original GRPO algorithm in Section 3.1, highlighting its *structural* components and computational demands. Next, in Section 3.2, we introduce the **PODS** (**P**olicy **O**ptimization with **D**own-**S**ampling) framework, which strategically selects informative rollouts to maximize hardware utilization during both inference and policy-update phases. In Section 3.3, we develop a principled *max-variance down-sampling* method that preserves strong contrastive signals, justified by Razin et al. (2025), by retaining only rollouts from the extremes of the reward spectrum. We show that this method admits an elegant, $O(n \log n)$ solution, making it practical for real-world deployment.

3.1 Preliminaries

Group Relative Policy Optimization (GRPO) (Shao et al., 2024) is a reinforcement-learning algorithm intended to enhance the reasoning capabilities of large language models (LLMs), particularly within the RLVR setting. Each GRPO training step follows a structured, two-phase process, described below.

Inference phase. Let π_θ denote the policy parameterized by θ, which defines a distribution over next-token probabilities given the previous tokens in a sequence. Given a single input prompt p (e.g., a math problem), GRPO first generates a group of n rollouts $\mathbf{o} = (o_1, o_2, \ldots, o_n)$ by autoregressively sampling from π_θ. Each rollout is a complete token sequence excluding the prompt, representing a possible solution. Each rollout is then evaluated using a reward model $r_i = R(o_i)$, which scores the quality and correctness of the corresponding output o_i. This yields a reward vector $\mathbf{r} = (r_1, r_2, \ldots, r_n)$. We then compute normalized advantage estimates: $a_i = (r_i - \mu)/\sigma$, where μ and σ are the mean and standard deviation of the rewards respectively.

Policy update phase. After computing the advantages, the policy is updated by optimizing the GRPO objective $L_{\text{GRPO}}(\theta)$. Specifically, for each rollout o_i with advantage a_i, we compute a loss for each token position t, and then average over all tokens and rollouts:

$$L_{\text{GRPO}}(\theta) = \frac{1}{n}\sum_{i=1}^{n}\frac{1}{|o_i|}\sum_{t=1}^{|o_i|} \min\left[\frac{\pi_\theta(o_{i,t} \mid p, o_{i,<t})}{\pi_{\theta_{\text{fixed}}}(o_{i,t} \mid p, o_{i,<t})} \cdot a_i,\ \text{clip}\left(\frac{\pi_\theta(o_{i,t} \mid p, o_{i,<t})}{\pi_{\theta_{\text{fixed}}}(o_{i,t} \mid p, o_{i,<t})}, 1-\epsilon, 1+\epsilon\right) \cdot a_i\right].$$

where $|o_i|$ is the number of tokens in o_i and $\pi_{\theta_{\text{fixed}}}$ is a frozen copy of the policy used for importance weighting. This asymmetric loss embodies the *slow to adopt, quick to abandon* learning principle—limiting how aggressively the policy increases probabilities for tokens in high-reward rollouts while allowing more substantial reductions for low-reward sequences.

3.2 PODS Framework

We propose to *decouple the inference and training phases* in GRPO. Rather than updating on every generated rollout, PODS first produces n rollouts in parallel and then trains on only a smaller subset of size $m < n$ selected by a down-sampling rule D. This strategy exploits parallelism during inference while substantially reducing the communication and memory costs of the subsequent policy update.

Definition 3.1 (Down-sampling rule)**.** *$D(\mathbf{o}, \mathbf{r}; m)$ is a function that takes n rollouts $\mathbf{o} = (o_1, o_2, \ldots, o_n)$, their corresponding rewards $\mathbf{r} = (r_1, r_2, \ldots, r_n)$, and the update size m. It outputs a subset of indices $S \subseteq \{1, 2, \ldots, n\}$, where $|S| = m$, indicating which rollouts to retain for the policy update phase.*

Given a selected subset of indices S, we compute the advantage estimates using only the selected rollouts: $a_{S,i} = (r_i - \mu_S)/\sigma_S$, where μ_S and σ_S are the mean and standard deviation of the rewards in the selected subset. The GRPO-PODS objective then becomes:

$$L_{\text{PODS}}(\theta, S) = \frac{1}{m} \sum_{i \in S} \frac{1}{|o_i|} \sum_{t=1}^{|o_i|} \min \left[\frac{\pi_\theta(o_{i,t} \mid p, o_{i,<t})}{\pi_{\theta_{\text{fixed}}}(o_{i,t} \mid p, o_{i,<t})} \cdot a_{S,i}, \text{clip} \left(\frac{\pi_\theta(o_{i,t} \mid p, o_{i,<t})}{\pi_{\theta_{\text{fixed}}}(o_{i,t} \mid p, o_{i,<t})}, 1 - \varepsilon, 1 + \varepsilon \right) \cdot a_{S,i} \right].$$

Algorithm 1 The PODS Framework for GRPO

Input: Models $\pi_\theta, \pi_{\theta_{\text{fixed}}}$, input prompt p, reward model R,
Number of rollouts n, update size m, down-sampling rule D

1: Independently sample n rollouts $\mathbf{o} = (o_1, o_2, \ldots, o_n)$ using $\pi_{\theta_{\text{fixed}}}$ for prompt p
2: Compute rewards $\mathbf{r} = (r_1, r_2, \ldots, r_n)$ using the reward model R
3: Down-sample a set of m rollouts $S \leftarrow D(\mathbf{o}, \mathbf{r}; m)$
4: Update the policy using the GRPO-PODS objective $L_{\text{PODS}}(\theta, S)$

Output: An updated model $\pi_{\theta_{\text{updated}}}$

Algorithm 1 outlines the PODS framework for GRPO with a single prompt p in a training iteration. When training on a batch of multiple prompts, we simply apply the same procedure to each prompt and then concatenate the down-sampled rollouts and rewards. We conclude this section by presenting two trivial down-sampling strategies that can potentially be applied within PODS.

Random down-sampling. The rule D_{rand} uniformly selects m indices from $\{1, 2, \ldots, n\}$ without replacement, thereby preserving the statistical properties of the original rollout distribution. In expectation, it yields the same parameter update as running standard GRPO on exactly m rollouts.

Percentile down-sampling. The rule D_{perc} selects the m rollouts by choosing the $\frac{0.5}{m}$, $\frac{1.5}{m}$, $\ldots$, $\frac{m-0.5}{m}$ quantiles of the reward distribution. This method ensures that the selected rollouts are evenly spaced across the reward spectrum, providing a more representative sample than random down-sampling.

Max-reward down-sampling. The rule D_{maxr} selects the m rollouts with the highest rewards, concentrating on examples that exhibit the most desirable behavior. This should allow the model to learn primarily from successful reasoning patterns. However, as we show in Section 4, ignoring low-reward rollouts deprives the policy of negative feedback and can significantly degrade performance.

3.3 Max-Variance Down-Sampling

We now introduce *max-variance down-sampling*, a principled down-sampling rule that selects the most diverse and informative rollouts according to their reward distribution.

Specifically, D_{maxv} chooses the subset S of size m that maximizes the empirical reward variance, i.e., $S = \arg\max_{|S|=m} \text{Var}(\{r_i \mid i \in S\})$. By spanning the full performance spectrum, it supplies strong contrastive signals between successful and unsuccessful reasoning paths. Recent work by Razin et al. (2025) provides an optimization-theoretic and empirical justification for this criterion.

A naive search would examine $O(\binom{n}{m})$ subsets. This is clearly infeasible for realistic n and m. We prove, however, that the optimal subset can be found in $O(n \log n)$ time.

Lemma 3.1. *For a sorted list of rewards $r_1 \leq r_2 \leq \cdots \leq r_n$, the variance-maximizing subset of size m always consists of the k highest rewards and $(m-k)$ lowest rewards for some $k \in \{0, 1, \ldots, m\}$. That is,*

$$\mathrm{Var}(\{r_1, \ldots, r_{m-k}\} \cup \{r_{n-k+1}, \ldots, r_n\}) = \max_{|S|=m} \mathrm{Var}(\{r_i \mid i \in S\}).$$

Proof of Lemma 3.1: Let $S^* = \arg\max_{|S|=m} \mathrm{Var}(\{r_i \mid i \in S\})$ be the optimal subset of size m. We will show that if S^* is not of the form $\{1, \ldots, m-k\} \cup \{n-k+1, \ldots, n\}$ for any k, then we can modify S^* to obtain a new subset S' of the same size with no smaller variance in rewards. By repeating this procedure, we can eventually reach a subset of this form.

Let μ be the mean of the rewards in S^*. Since S^* does not take the form of $\{1, \ldots, m-k\} \cup \{n-k+1, \ldots, n\}$ for any k, there exists either (i) an element $i \in S^*$ such that $i > 1, r_i \leq \mu$ and $i-1 \notin S^*$, or (ii) an element $j \in S^*$ such that $j < n, r_j \geq \mu$ and $j+1 \notin S^*$. That is, there exists an element in S^*, such that another element further from μ is not in S^*. We will show that we can swap them without decreasing variance.

For the ease of notation, we will denote $\mathrm{Var}(\{r_i \mid i \in S\})$ as $\mathrm{Var}(S)$ in this proof.

For case (i), let $S' = (S^* \setminus \{i\}) \cup \{i-1\}$, and let μ' be the mean of the rewards in S'. Then

$$\begin{aligned}
\mathrm{Var}(S') - \mathrm{Var}(S^*) &= \left(\frac{1}{m}\sum_{t \in S'} r_t^2 - \mu'^2\right) - \left(\frac{1}{m}\sum_{t \in S^*} r_t^2 - \mu^2\right) \\
&= \frac{1}{m}(r_{i-1}^2 - r_i^2) - (\mu'^2 - \mu^2) \\
&= \frac{1}{m}(r_{i-1} - r_i)(r_{i-1} + r_i) - (\mu' - \mu)(\mu' + \mu) \\
&= \frac{1}{m}(r_{i-1} - r_i)[(r_{i-1} + r_i) - (\mu' + \mu)] \geq 0.
\end{aligned}$$

For case (ii), let $S' = (S^* \setminus \{j\}) \cup \{j+1\}$, we can similarly show that $\mathrm{Var}(S') - \mathrm{Var}(S^*) \geq 0$.

In either case, we have shown that we can modify S^* to obtain a new subset S' of the same size that has no smaller variance in rewards. We can repeat this process until we reach a subset of the form $\{1, \ldots, m-k\} \cup \{n-k+1, \ldots, n\}$ for some k. Thus, we conclude that there must exist one optimal subset of this form for some k. ■

Lemma 3.1 naturally leads to a practical algorithm, Algorithm 2, for max-variance down-sampling. Moreover, it also offers intuition as to why maximizing variance is effective: the optimal subset contains the k highest and the $(m-k)$ lowest rewards, capturing contrastive signals from both positive and negative examples.

Algorithm 2 Max-Variance Down-Sampling

Input: Number of rollouts n, update size m, rollouts $\{o_1, o_2, \ldots, o_n\}$, rewards $\{r_1, r_2, \ldots, r_n\}$
1: Sort the rollouts by reward and get the sorted indices $ind \leftarrow \mathrm{argsort}(\{r_1, r_2, \ldots, r_n\})$
2: Let $S_{\text{ans}} \leftarrow \{ind_1, \ldots, ind_m\}$
3: **for** $k \in \{1, \ldots, m\}$ **do**
4: Let $S_{\text{this}} \leftarrow \{ind_1, \ldots, ind_{m-k}\} \cup \{ind_{n-k+1}, \ldots, ind_n\}$
5: Let $S_{\text{ans}} \leftarrow S_{\text{this}}$ **if** $\mathrm{Var}(\{r_i \mid i \in S_{\text{this}}\}) > \mathrm{Var}(\{r_i \mid i \in S_{\text{ans}}\})$
6: **end for**
Output: Selected indices S_{ans} of rollouts

Theorem 1. *Algorithm 2 computes the max-variance down-sampling rule correctly. Moreover, it can be implemented in $O(n \log n)$ time.*

Proof of Theorem 1: The correctness of Algorithm 2 follows directly from Lemma 3.1.

For the time complexity, we first sort the rewards in $O(n \log n)$ time. To compute the variance of the selected rollouts, note that $\mathrm{Var}(\{x \mid x \in S_{\text{this}}\}) = \mathbf{E}_{x \in S_{\text{this}}}[x^2] - (\mathbf{E}_{x \in S_{\text{this}}}[x])^2$. We can maintain the

prefix sums of the rewards and the squared rewards in $O(n)$ time. Then, for each k, we can compute the variance of the selected rollouts in $O(1)$ time using the prefix sums. Thus, the overall time complexity is $O(n \log n) + O(m) = O(n \log n)$. ■

Theorem 1 shows that the max-variance down-sampling rule can be computed efficiently, which enables its practical application in GRPO-PODS. We conclude this section by noting an important special case of the max-variance down-sampling rule.

Theorem 2. *Let m be an even integer. When the rewards are binary, selecting $m/2$ rollouts with the highest rewards and $m/2$ rollouts with the lowest rewards maximizes the variance of the rewards.*

Proof of Theorem 2: Let the number of rollouts with reward 1 be k. Then, the number of rollouts with reward 0 is $n - k$. If $k \leq m/2$, then any subset of m rollouts contains at most k rollouts with reward 1, and the variance is maximized by selecting these k rollouts and any $(m - k)$ rollouts with reward 0. If $n - k \leq m/2$, then any subset of m rollouts contains at most $(n - k)$ rollouts with reward 0, and the variance is maximized by selecting these $(n - k)$ rollouts and any $m - (n - k)$ rollouts with reward 1. Otherwise, any subset of $m/2$ rollouts with reward 1 and $m/2$ rollouts with reward 0 maximizes the variance. In all cases, we can select $m/2$ rollouts with the highest rewards and $m/2$ rollouts with the lowest rewards to maximize the variance. This concludes the proof. ■

4 Experiments

We evaluate PODS across diverse hardware configurations, model architectures, and model scales to demonstrate its generalizability and practical benefits. We test on three reasoning benchmarks of different domains, GSM8K (Cobbe et al., 2021), MATH (Hendrycks et al., 2021) and the L3 Chemistry subset of SciKnowEval (Feng et al., 2024), using Qwen2.5 (Qwen et al., 2025) and Llama3.2 (MetaAI, 2024) models ranging from 3B to 7B parameters. Our experimental design covers both resource-constrained single-GPU setups and multi-GPU distributed training to validate PODS across different deployment scenarios. Table 1 describes our experimental configurations. We publish the code for our experiments at https://github.com/YixuanEvenXu/pods.

Setting	Benchmark	Model	Parameters	GPUs	Fine-tuning Method
(a)	GSM8K	Qwen2.5	3B	1 L40S	LoRA (rank 64, $\alpha = 64$)
(b)	GSM8K	Llama3.2	3B	1 L40S	LoRA (rank 64, $\alpha = 64$)
(c)	MATH	Qwen2.5	3B	1 L40S	LoRA (rank 64, $\alpha = 64$)
(d)	Chemistry	Qwen2.5	3B	1 L40S	LoRA (rank 64, $\alpha = 64$)
(e)	GSM8K	Qwen2.5	3B	8 H100s	Full-Parameter
(f)	GSM8K	Qwen2.5	7B	8 A100s	Full-Parameter

Table 1: Experimental configurations testing GRPO with PODS across task domains, model scales, hardware constraints, and training paradigms. Settings (a-d) test resource-constrained scenarios with LoRA fine-tuning, while (e-f) evaluate full-parameter training with distributed setups.

Training infrastructure. For settings (a-d), we use `Unsloth` (Daniel Han & team, 2023) with `TRL` (von Werra et al., 2020) for efficient LoRA (Hu et al., 2022) reinforcement learning. For settings (e-f), we implement distributed training with `DeepSpeed ZeRO-2` (Rajbhandari et al., 2020) and extend the `open-r1` library (HuggingFace, 2025) to support PODS on multiple devices.

Rewards and evaluations. We employ rule-based reward models that score rollouts, following standard practices in reasoning evaluation. Specifically, we reward an answer for correctness, format compliance, and the right number of thinking tags separately, resulting in a discrete but non-binary reward function. We provide additional details about the reward models Appendix A.1.

Section roadmap. In Section 4.1, we compare the performance of GRPO and GRPO-PODS across six hardware and model settings listed in Table 1. We show that for all the settings we test, GRPO-PODS

consistently outperforms GRPO in terms of test performance throughout the training. Then, in Section 4.2, we focus on setting (a), and analyze the effect of the rollout and update sizes (n, m) on the performance of GRPO-PODS, providing empirical insights into how to choose the rollout and update sizes for GRPO-PODS. We also present additional experiments about different down-sampling rules (Section 4.3) and different design choices of advantage normalization (Appendix A.3), additional evaluation results about PODS' speed up ratio compared to GRPO (Appendix A.4) and test performance generalization across different test sets (Appendix A.5), and the average response length over the course of training (Appendix A.6).

4.1 Comparing GRPO-PODS to baseline GRPO

We evaluate max-variance down-sampling PODS with GRPO against baseline GRPO using two experimental designs reflecting real-world constraints. For single-GPU settings (a-d), we compare against vanilla GRPO with the same training batch sizes (m), where m is selected so that one training batch fits within GPU memory. This corresponds to the comparison between the first and the third rows in Fig. 2. For distributed settings (e-f), we compare against GRPO with gradient accumulation (GRPO-GA), the standard approach for scaling RLVR. In GRPO-GA, large training batches are processed through multiple gradient accumulation steps, enabling updating on larger effective batch sizes at the cost of increased communication overhead and iteration time. We fix the total rollouts generated per prompt (n) and compare GRPO-GA against GRPO-PODS. This corresponds to the comparison between the second and the third rows in Fig. 2. The detailed hyperparameters used for our experiments are listed in Appendix A.2.

Fig. 3 shows test accuracy over wall-clock training time across all experiment configurations. PODS consistently achieves faster convergence: reaching the baselines' peak accuracies at least 1.7× faster (see Appendix A.4 for complete results) while often converging to a higher final performance. These results demonstrate PODS' broad applicability across task domains (Math and Chemistry), model scales (3B-7B), architectures (Qwen2.5, Llama3.2), and deployment scenarios, making it a practical improvement for RLVR systems using GRPO.

4.2 Effect of Rollout and Update Sizes (n, m)

A key practical question for PODS adoption is how to choose the rollout size (n) and training batch size (m). While a larger n provides more diverse rollouts for selection, it also increases inference costs. Meanwhile, a smaller m reduces update costs but may provide insufficient training signal. As shown in Fig. 4, we study these trade-offs on experimental setting (a) to provide deployment guidance.

Increasing rollout size n exhibits diminishing returns with an optimal point around $n = 64$. Performance initially improves as larger pools enable better sample selection, but degrades beyond $n = 128$ due to two factors: (1) inference runtime grows significantly as GPU memory saturates, and (2) marginal improvements in rollout diversity plateau while computational overhead continues rising.

Training batch size m shows robust performance across a wide range, with minimal degradation until very small values ($m \leq 4$). This suggests PODS' max-variance selection maintains effective learning signals even with aggressive down-sampling ratios up to 16 where $n = 64, m = 4$.

Practical guidelines. These results suggest down-sampling ratio of 2 to 4 provides an effective balance of performance and efficiency. For resource-constrained settings, aggressive down-sampling ratios up to 16 remain viable, while memory-rich environments can benefit from larger rollout pools up to hardware limits.

4.3 Comparing Different Down-Sampling Rules

We study the effect of different down-sampling rules on the performance of GRPO-PODS in this section. We conduct experiments on experimental setting (a). We compare four different down-sampling rules: (1) max-variance down-sampling, (2) max-reward down-sampling, (3) random down-sampling, and (4) percentile down-sampling. The results are shown in Fig. 5. We observe that the max-variance down-sampling rule consistently outperforms the other down-sampling rules throughout the training. This indicates that the max-variance down-sampling rule is effective in selecting informative rollouts for training.

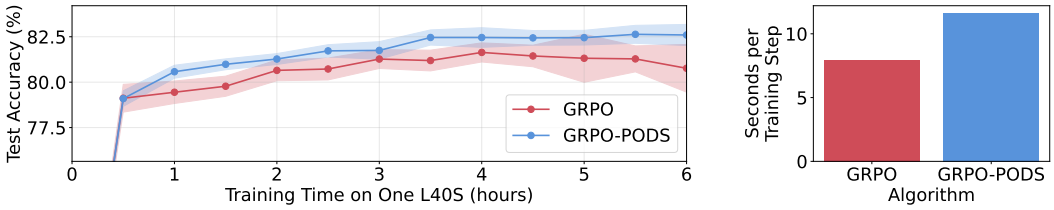

(a) Training Qwen2.5 (3B) on GSM8K with one L40S GPU

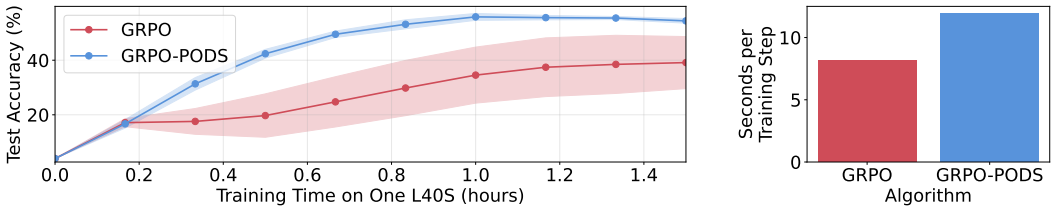

(b) Training Llama3.2 (3B) on GSM8K with one L40S GPU

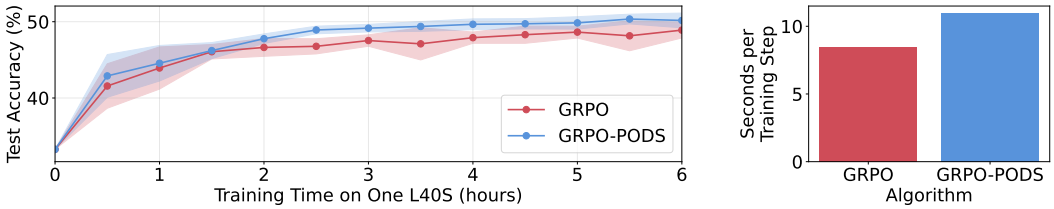

(c) Training Qwen2.5 (3B) on MATH with one L40S GPU

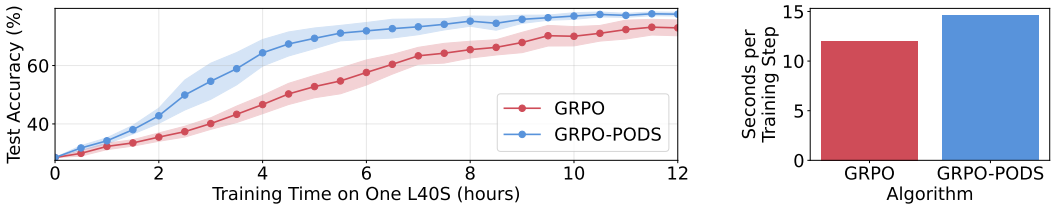

(d) Training Qwen2.5 (3B) on Chemistry with one L40S GPU

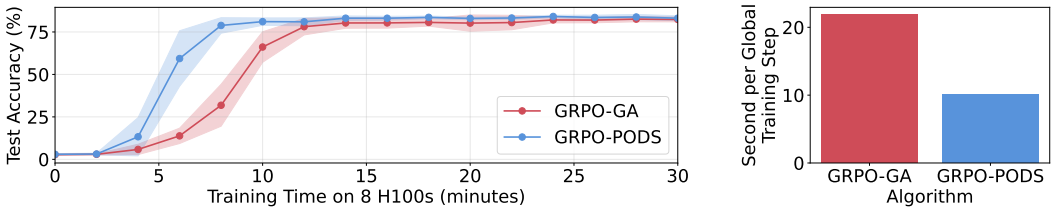

(e) Training Qwen2.5 (3B) on GSM8K with 8 H100 GPUs

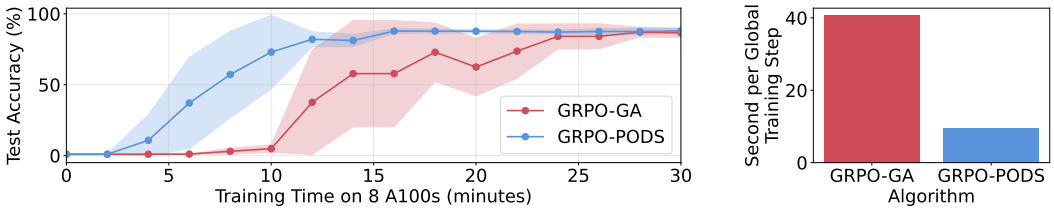

(f) Training Qwen2.5 (7B) on GSM8K with 8 A100 GPUs

Figure 3: Performance and per-step run time comparison of standard GRPO and GRPO-PODS with max-variance down-sampling across different datasets and hardware environments. For the performance comparison, the x-axis shows the training time, and the y-axis shows the accuracy on the test set. The shaded area represents 1.96 times the standard error of the mean.

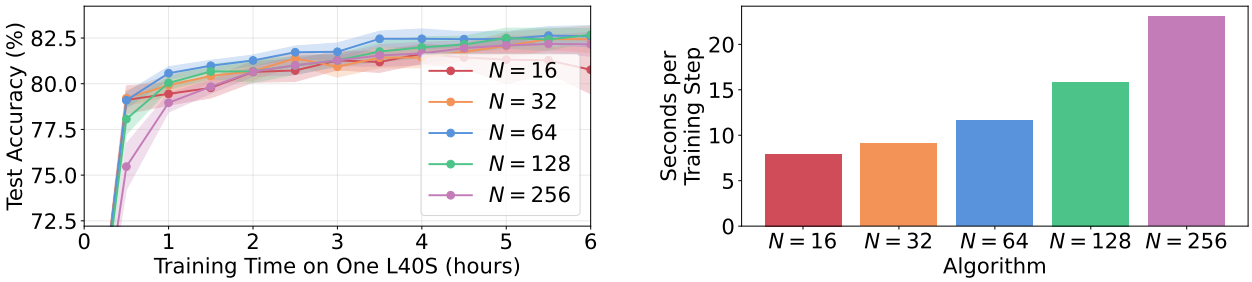

(a) Fixing $m = 16$ and varying $n \in \{16, 32, 64, 128, 256\}$

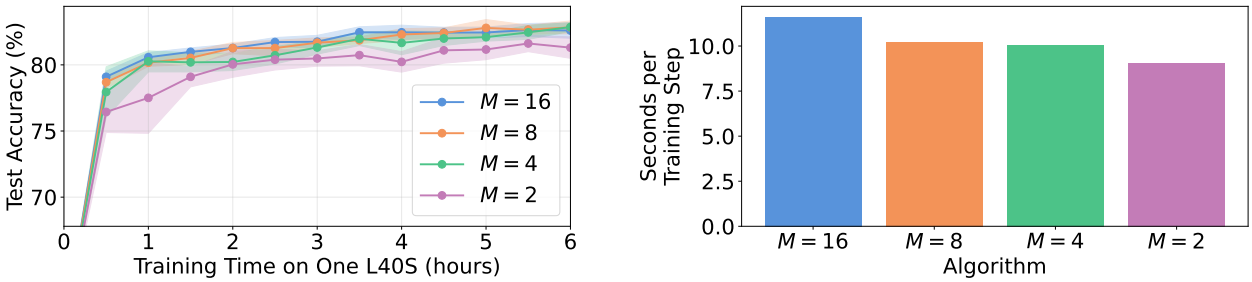

(b) Fixing $n = 64$ and varying $m \in \{16, 8, 4, 2\}$

Figure 4: Performance and per-step run time comparison of GRPO-PODS with max-variance down-sampling across different settings of n and m. The training is conducted on the GSM8K dataset with one L40S. For the performance comparison, the x-axis shows the training time, and the y-axis shows the accuracy on the test set. The shaded area represents 1.96 times the standard error of the mean.

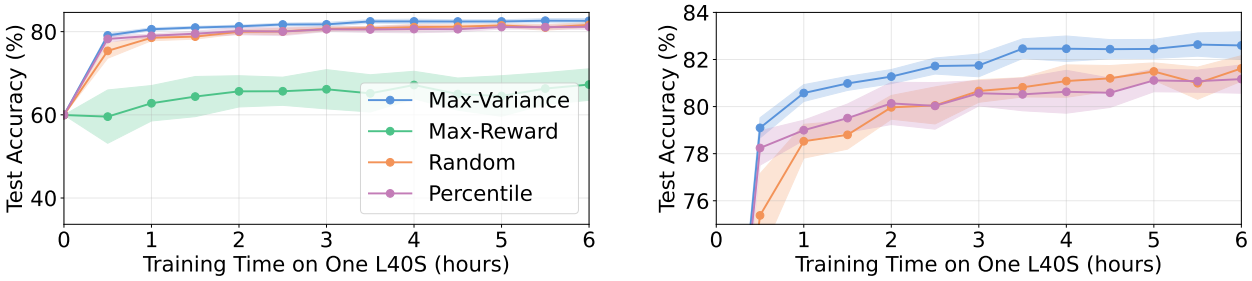

Figure 5: Performance of GRPO-PODS with the max-variance, max-reward, random and percentile down-sampling rules. The training is conducted on the GSM8K dataset with one L40S. The x-axis shows the training time, and the y-axis shows the accuracy on the test set. The shaded area represents 1.96 times the standard error of the mean. The right panel shows a Zoomed-in view of the left one.

5 Conclusion and Discussion

We introduced **PODS**, a lightweight framework that addresses a fundamental bottleneck in modern RLVR training: the asymmetry between embarrassingly parallel rollout generation and memory-intensive policy updates. PODS generates large batches of rollouts in parallel and updates the policy on only an informative subset chosen by the max-variance rule. Our analysis shows that the optimal subset can be found in $O(n \log n)$ time. This simple yet principled approach consistently outperforms standard GRPO under equal wall-clock budgets, delivers at least a 1.7× speedup and reaching higher final accuracy across diverse model architectures, scales, and deployment scenarios. Our ablation study shows that the performance of PODS is robust over a wide range of down-sampling ratios provided m is not too small, empirically confirming our method's efficacy.

Limitations. As we emphasize in the paper, our evaluation focuses on RLVR tasks where response correctness is verifiable. Other domains such as open-ended dialogue may exhibit distinct dynamics of the

algorithms. Moreover, in workloads that demand greater prompt diversity, similar gains might be obtained by processing more prompts per iteration with fewer rollouts per prompt and accumulating gradients across prompts, which is an alternative path to address the inference-update asymmetry. Finally, because PODS alters the training rollout distribution through selective down-sampling, it behaves off-policy and may be unsuitable when strict on-policy guarantees are required despite its improved empirical performance.

Scope of claims. Our empirical and theoretical claims in this paper are specific to PODS instantiated within GRPO. While we expect the inference-update asymmetry to be present in other RLVR pipelines, demonstrating that down-sampling yields comparable benefits for other RL methods (e.g., PPO-style objectives or value-based variants) requires separate analysis and experimentation.

Discussion and future work. PODS is a general framework that admits different down-sampling rules. In this paper, we focus on the max-variance rule due to its superior empirical performance in common RLVR settings. In some scenarios, other rules might be more effective. For example, when different prompts cause the model to have highly varying reward distributions, applying the max-variance rule across all rollouts may lead to over-sampling from a small subset of prompts with extreme difficulty levels. In such cases, applying the max-variance rule within each prompt and then selecting a balanced subset across prompts may be more effective. More broadly, the down-sampling rule can be designed to take into account more information beyond the reward values, such as the rollouts' entropy, similarity measures between rollouts, or even a target reward distribution that we wish to down-sample towards. Exploring these alternative down-sampling rules and their empirical performance across different settings is an interesting direction for future work.

References

Chenxin An, Zhihui Xie, Xiaonan Li, Lei Li, Jun Zhang, Shansan Gong, Ming Zhong, Jingjing Xu, Xipeng Qiu, Mingxuan Wang, and Lingpeng Kong. Polaris: A post-training recipe for scaling reinforcement learning on advanced reasoning models, 2025. URL `https://hkunlp.github.io/blog/2025/Polaris`.

William Bankes, George Hughes, Ilija Bogunovic, and Zi Wang. Reducr: Robust data downsampling using class priority reweighting. *Advances in Neural Information Processing Systems*, 37:82781–82810, 2024.

Xiaohui Bei, Nick Gravin, Pinyan Lu, and Zhihao Gavin Tang. Bidder subset selection problem in auction design. In *Proceedings of the 2023 Annual ACM-SIAM Symposium on Discrete Algorithms (SODA)*, pp. 3788–3801. SIAM, 2023.

Zhipeng Chen, Yingqian Min, Beichen Zhang, Jie Chen, Jinhao Jiang, Daixuan Cheng, Wayne Xin Zhao, Zheng Liu, Xu Miao, Yang Lu, et al. An empirical study on eliciting and improving r1-like reasoning models. *arXiv preprint arXiv:2503.04548*, 2025.

Kenneth L Clarkson. Coresets, sparse greedy approximation, and the frank-wolfe algorithm. *ACM Transactions on Algorithms (TALG)*, 6(4):1–30, 2010.

Karl Cobbe, Vineet Kosaraju, Mohammad Bavarian, Mark Chen, Heewoo Jun, Lukasz Kaiser, Matthias Plappert, Jerry Tworek, Jacob Hilton, Reiichiro Nakano, et al. Training verifiers to solve math word problems. *arXiv preprint arXiv:2110.14168*, 2021.

Ganqu Cui, Lifan Yuan, Zefan Wang, Hanbin Wang, Wendi Li, Bingxiang He, Yuchen Fan, Tianyu Yu, Qixin Xu, Weize Chen, et al. Process reinforcement through implicit rewards. *arXiv preprint arXiv:2502.01456*, 2025.

Marco Cusumano-Towner, David Hafner, Alex Hertzberg, Brody Huval, Aleksei Petrenko, Eugene Vinitsky, Erik Wijmans, Taylor Killian, Stuart Bowers, Ozan Sener, et al. Robust autonomy emerges from self-play. *arXiv preprint arXiv:2502.03349*, 2025.

Michael Han Daniel Han and Unsloth team. Unsloth, 2023. URL `http://github.com/unslothai/unsloth`.

Meta Fundamental AI Research Diplomacy Team FAIR, Anton Bakhtin, Noam Brown, Emily Dinan, Gabriele Farina, Colin Flaherty, Daniel Fried, Andrew Goff, Jonathan Gray, Hengyuan Hu, et al. Human-level play

in the game of diplomacy by combining language models with strategic reasoning. *Science*, 378(6624): 1067–1074, 2022.

Kehua Feng, Xinyi Shen, Weijie Wang, Xiang Zhuang, Yuqi Tang, Qiang Zhang, and Keyan Ding. Sciknoweval: Evaluating multi-level scientific knowledge of large language models. *arXiv preprint arXiv:2406.09098*, 2024.

Samir Yitzhak Gadre, Gabriel Ilharco, Alex Fang, Jonathan Hayase, Georgios Smyrnis, Thao Nguyen, Ryan Marten, Mitchell Wortsman, Dhruba Ghosh, Jieyu Zhang, et al. Datacomp: In search of the next generation of multimodal datasets. *Advances in Neural Information Processing Systems*, 36:27092–27112, 2023.

Zitian Gao, Boye Niu, Xuzheng He, Haotian Xu, Hongzhang Liu, Aiwei Liu, Xuming Hu, and Lijie Wen. Interpretable contrastive monte carlo tree search reasoning. *arXiv preprint arXiv:2410.01707*, 2024.

Sachin Goyal, Pratyush Maini, Zachary C Lipton, Aditi Raghunathan, and J Zico Kolter. Scaling laws for data filtering–data curation cannot be compute agnostic. In *Proceedings of the IEEE/CVF Conference on Computer Vision and Pattern Recognition*, pp. 22702–22711, 2024.

Nikolai Gravin, Yixuan Even Xu, and Renfei Zhou. Bidder selection problem in position auctions: A fast and simple algorithm via poisson approximation. In *Proceedings of the ACM Web Conference 2024*, pp. 89–98, 2024.

Daya Guo, Dejian Yang, Haowei Zhang, Junxiao Song, Ruoyu Zhang, Runxin Xu, Qihao Zhu, Shirong Ma, Peiyi Wang, Xiao Bi, et al. Deepseek-r1: Incentivizing reasoning capability in llms via reinforcement learning. *arXiv preprint arXiv:2501.12948*, 2025.

Sariel Har-Peled and Soham Mazumdar. On coresets for k-means and k-median clustering. In *Proceedings of the thirty-sixth annual ACM symposium on Theory of computing*, pp. 291–300, 2004.

Dan Hendrycks, Collin Burns, Saurav Kadavath, Akul Arora, Steven Basart, Eric Tang, Dawn Song, and Jacob Steinhardt. Measuring mathematical problem solving with the math dataset. *NeurIPS*, 2021.

Yuenan Hou, Lifeng Liu, Qing Wei, Xudong Xu, and Chunlin Chen. A novel ddpg method with prioritized experience replay. In *2017 IEEE international conference on systems, man, and cybernetics (SMC)*, pp. 316–321. IEEE, 2017.

Edward J Hu, Yelong Shen, Phillip Wallis, Zeyuan Allen-Zhu, Yuanzhi Li, Shean Wang, Lu Wang, Weizhu Chen, et al. Lora: Low-rank adaptation of large language models. *ICLR*, 1(2):3, 2022.

Jian Hu. Reinforce++: A simple and efficient approach for aligning large language models. *arXiv preprint arXiv:2501.03262*, 2025.

Jingcheng Hu, Yinmin Zhang, Qi Han, Daxin Jiang, Xiangyu Zhang, and Heung-Yeung Shum. Open-reasoner-zero: An open source approach to scaling up reinforcement learning on the base model. *arXiv preprint arXiv:2503.24290*, 2025.

HuggingFace. Open r1: A fully open reproduction of deepseek-r1, January 2025. URL `https://github.com/huggingface/open-r1`.

Aaron Jaech, Adam Kalai, Adam Lerer, Adam Richardson, Ahmed El-Kishky, Aiden Low, Alec Helyar, Aleksander Madry, Alex Beutel, Alex Carney, et al. Openai o1 system card. *arXiv preprint arXiv:2412.16720*, 2024.

Vishal Kaushal, Rishabh Iyer, Suraj Kothawade, Rohan Mahadev, Khoshrav Doctor, and Ganesh Ramakrishnan. Learning from less data: A unified data subset selection and active learning framework for computer vision. In *2019 IEEE Winter Conference on Applications of Computer Vision (WACV)*, pp. 1289–1299. IEEE, 2019.

Amirhossein Kazemnejad, Milad Aghajohari, Eva Portelance, Alessandro Sordoni, Siva Reddy, Aaron Courville, and Nicolas Le Roux. Vineppo: Unlocking rl potential for llm reasoning through refined credit assignment. *arXiv preprint arXiv:2410.01679*, 2024.

Mu Li, Gary L Miller, and Richard Peng. Iterative row sampling. In *2013 IEEE 54th Annual Symposium on Foundations of Computer Science*, pp. 127–136. IEEE, 2013.

Yuzong Liu, Rishabh K Iyer, Katrin Kirchhoff, and Jeff A Bilmes. Svitchboard ii and fisver i: high-quality limited-complexity corpora of conversational english speech. In *INTERSPEECH*, pp. 673–677, 2015.

MetaAI. Llama 3.2: Revolutionizing edge ai and vision with open, customizable models. `https://ai.meta.com/blog/llama-3-2-connect-2024-vision-edge-mobile-devices/`, 2024. Accessed: 2025-09-23.

OpenAI. Learning to reason with language models. `https://openai.com/index/learning-to-reason-with-llms`, 2024.

Long Ouyang, Jeffrey Wu, Xu Jiang, Diogo Almeida, Carroll Wainwright, Pamela Mishkin, Chong Zhang, Sandhini Agarwal, Katarina Slama, Alex Ray, et al. Training language models to follow instructions with human feedback. *Advances in neural information processing systems*, 35:27730–27744, 2022.

Qwen, An Yang, Baosong Yang, Beichen Zhang, Binyuan Hui, Bo Zheng, Bowen Yu, Chengyuan Li, Dayiheng Liu, Fei Huang, Haoran Wei, Huan Lin, Jian Yang, Jianhong Tu, Jianwei Zhang, Jianxin Yang, Jiaxi Yang, Jingren Zhou, Junyang Lin, Kai Dang, Keming Lu, Keqin Bao, Kexin Yang, Le Yu, Mei Li, Mingfeng Xue, Pei Zhang, Qin Zhu, Rui Men, Runji Lin, Tianhao Li, Tianyi Tang, Tingyu Xia, Xingzhang Ren, Xuancheng Ren, Yang Fan, Yang Su, Yichang Zhang, Yu Wan, Yuqiong Liu, Zeyu Cui, Zhenru Zhang, and Zihan Qiu. Qwen2.5 technical report, 2025. URL `https://arxiv.org/abs/2412.15115`.

Samyam Rajbhandari, Jeff Rasley, Olatunji Ruwase, and Yuxiong He. Zero: Memory optimizations toward training trillion parameter models. In *SC20: International Conference for High Performance Computing, Networking, Storage and Analysis*, pp. 1–16. IEEE, 2020.

Noam Razin, Zixuan Wang, Hubert Strauss, Stanley Wei, Jason D Lee, and Sanjeev Arora. What makes a reward model a good teacher? an optimization perspective. *arXiv preprint arXiv:2503.15477*, 2025.

Mark Rudelson and Roman Vershynin. Sampling from large matrices: An approach through geometric functional analysis. *Journal of the ACM (JACM)*, 54(4):21–es, 2007.

Baturay Saglam, Furkan B Mutlu, Dogan C Cicek, and Suleyman S Kozat. Actor prioritized experience replay. *Journal of Artificial Intelligence Research*, 78:639–672, 2023.

Tom Schaul, John Quan, Ioannis Antonoglou, and David Silver. Prioritized experience replay. *arXiv preprint arXiv:1511.05952*, 2015.

Christoph Schuhmann, Richard Vencu, Romain Beaumont, Robert Kaczmarczyk, Clayton Mullis, Aarush Katta, Theo Coombes, Jenia Jitsev, and Aran Komatsuzaki. Laion-400m: Open dataset of clip-filtered 400 million image-text pairs. *arXiv preprint arXiv:2111.02114*, 2021.

John Schulman, Filip Wolski, Prafulla Dhariwal, Alec Radford, and Oleg Klimov. Proximal policy optimization algorithms. *arXiv preprint arXiv:1707.06347*, 2017.

Zhihong Shao, Peiyi Wang, Qihao Zhu, Runxin Xu, Junxiao Song, Xiao Bi, Haowei Zhang, Mingchuan Zhang, YK Li, Y Wu, et al. Deepseekmath: Pushing the limits of mathematical reasoning in open language models. *arXiv preprint arXiv:2402.03300*, 2024.

Nisan Stiennon, Long Ouyang, Jeffrey Wu, Daniel Ziegler, Ryan Lowe, Chelsea Voss, Alec Radford, Dario Amodei, and Paul F Christiano. Learning to summarize with human feedback. *Advances in neural information processing systems*, 33:3008–3021, 2020.

Leandro von Werra, Younes Belkada, Lewis Tunstall, Edward Beeching, Tristan Thrush, Nathan Lambert, Shengyi Huang, Kashif Rasul, and Quentin Gallouédec. Trl: Transformer reinforcement learning. `https://github.com/huggingface/trl`, 2020.

Kai Wei, Yuzong Liu, Katrin Kirchhoff, and Jeff Bilmes. Unsupervised submodular subset selection for speech data. In *2014 IEEE International Conference on Acoustics, Speech and Signal Processing (ICASSP)*, pp. 4107–4111. IEEE, 2014.

Yuxi Xie, Anirudh Goyal, Wenyue Zheng, Min-Yen Kan, Timothy P Lillicrap, Kenji Kawaguchi, and Michael Shieh. Monte carlo tree search boosts reasoning via iterative preference learning. *arXiv preprint arXiv:2405.00451*, 2024.

Wei Xiong, Jiarui Yao, Yuhui Xu, Bo Pang, Lei Wang, Doyen Sahoo, Junnan Li, Nan Jiang, Tong Zhang, Caiming Xiong, et al. A minimalist approach to llm reasoning: from rejection sampling to reinforce. *arXiv preprint arXiv:2504.11343*, 2025.

Qiying Yu, Zheng Zhang, Ruofei Zhu, Yufeng Yuan, Xiaochen Zuo, Yu Yue, Tiantian Fan, Gaohong Liu, Lingjun Liu, Xin Liu, et al. Dapo: An open-source llm reinforcement learning system at scale. *arXiv preprint arXiv:2503.14476*, 2025.

Yufeng Yuan, Qiying Yu, Xiaochen Zuo, Ruofei Zhu, Wenyuan Xu, Jiaze Chen, Chengyi Wang, TianTian Fan, Zhengyin Du, Xiangpeng Wei, et al. Vapo: Efficient and reliable reinforcement learning for advanced reasoning tasks. *arXiv preprint arXiv:2504.05118*, 2025a.

Yufeng Yuan, Yu Yue, Ruofei Zhu, Tiantian Fan, and Lin Yan. What's behind ppo's collapse in long-cot? value optimization holds the secret. *arXiv preprint arXiv:2503.01491*, 2025b.

Xiaojiang Zhang, Jinghui Wang, Zifei Cheng, Wenhao Zhuang, Zheng Lin, Minglei Zhang, Shaojie Wang, Yinghan Cui, Chao Wang, Junyi Peng, et al. Srpo: A cross-domain implementation of large-scale reinforcement learning on llm. *arXiv preprint arXiv:2504.14286*, 2025.

Haizhong Zheng, Yang Zhou, Brian R Bartoldson, Bhavya Kailkhura, Fan Lai, Jiawei Zhao, and Beidi Chen. Act only when it pays: Efficient reinforcement learning for llm reasoning via selective rollouts. *arXiv preprint arXiv:2506.02177*, 2025.

Daniel M Ziegler, Nisan Stiennon, Jeffrey Wu, Tom B Brown, Alec Radford, Dario Amodei, Paul Christiano, and Geoffrey Irving. Fine-tuning language models from human preferences. *arXiv preprint arXiv:1909.08593*, 2019.

A Additional Experimental Details

A.1 Reward Functions

We list the reward functions we use in our experiments below.

Accuracy (1 for correct, 0 for incorrect): For mathematical reasoning tasks, we use a binary reward indicating whether the final answer is correct. This is computed by comparing the model's final answer to the ground truth solution using LaTeX parsing and symbolic verification, which allows for robust equivalence checking even when the model's answer is not in the exact same format as the ground truth. For Chemistry problems, the answer is always a letter in {A, B, C, D}, so we can directly compare with the correct answer.

Format (1 for compliant, 0 for non-compliant): For a response to be considered format-compliant, it must follow the exact XML structure we specify for reasoning and answer. This requires reasoning to be enclosed within `<think>` tags and the final answer within `<answer>` tags, following the exact pattern `<think>\n...\n</think>\n<answer>\n...\n</answer>`.

Tag count (0 to 1 partial credit): The model receives 0.25 points each for correct placement of `<think>\n`, `\n</think>\n`, `\n<answer>\n`, and `\n</answer>` tags. We allow partial credit for partially correct formatting.

A.2 Hyperparameters

In Table 2, we list the key hyperparameters we use for different experimental settings.

Table 2: Hyperparameters for different experimental settings.

Setting	**(a)**	**(b)**	**(c)**	**(d)**	**(e)**	**(f)**
Optimizer	AdamW	AdamW	AdamW	AdamW	AdamW	AdamW
Max Sequence Length	1024	1024	1024	1024	2048	2048
Lora Rank	64	64	64	64	N/A	N/A
Lora Alpha	64	64	64	64	N/A	N/A
KL Coefficient	0.00	0.04	0.00	0.00	0.00	0.00
Learning Rate	$5 \cdot 10^{-6}$	$2 \cdot 10^{-6}$	$5 \cdot 10^{-6}$	$5 \cdot 10^{-6}$	$2 \cdot 10^{-5}$	$1.5 \cdot 10^{-5}$
Weight Decay	0.1	0.1	0.1	0.1	0.1	0.1
Grad Clipping	1.0	1.0	1.0	1.0	1.0	1.0
GA Steps (GRPO-PODS)	1	1	1	1	4	4
Rollout Batch Size (GRPO-PODS)	64	64	32	64	128	128
Update Batch Size (GRPO-PODS)	16	16	8	16	32	32
Effective n (GRPO-PODS)	64	64	32	64	512	512
Effective m (GRPO-PODS)	16	16	8	16	128	128
Down-Sampling Ratio	4	4	4	4	4	4
GA Steps (GRPO)	1	1	1	1	N/A	N/A
Rollout Batch Size (GRPO)	16	8	16	16	N/A	N/A
Update Batch Size (GRPO)	16	8	16	16	N/A	N/A
Effective n (GRPO)	16	8	16	16	N/A	N/A
Effective m (GRPO)	16	8	16	16	N/A	N/A
GA Steps (GRPO-GA)	N/A	N/A	N/A	N/A	16	16
Rollout Batch Size (GRPO-GA)	N/A	N/A	N/A	N/A	32	32
Update Batch Size (GRPO-GA)	N/A	N/A	N/A	N/A	32	32
Effective n (GRPO-GA)	N/A	N/A	N/A	N/A	512	512
Effective m (GRPO-GA)	N/A	N/A	N/A	N/A	512	512

Note on gradient accumulation. For experiment settings (e) and (f), we ensure a fair comparison between GRPO-PODS and GRPO-GA by matching the total number of rollouts (effective n) generated per

prompt. This is done by equating the product of rollout batch size and GA steps across both methods. In the `open-r1` implementation, GA steps determine both rollout generation and training updates. For example, with rollout batch size 128 and GA steps 4, the effective n is $128 \times 4 = 512$. We fixed this number at 512 for both GRPO-PODS and GRPO-GA. For GRPO-PODS, each rollout batch is down-sampled by a factor of 4, resulting in an update batch size of 32 and an effective m of $32 \times 4 = 128$. Because down-sampling is applied directly after generating each batch rather than after aggregation, GRPO-GA must increase GA steps by 4× (from 4 to 16) to maintain the same effective n. This adjustment ensures that both variants process an equal number of rollouts while respecting their structural differences.

A.3 On Advantage Normalization

In Section 3.2, we mention that in GRPO-PODS, we first apply the down-sampling to the rollout batch, and then compute the advantage normalization statistics (mean and standard deviation) using the down-sampled batch. This design ensures the advantage normalization is consistent with the actual data used for policy updates, so that each update batch has a total advantage of 0. In this section, we study the effect of this design choice by comparing it with an alternative design where the advantage normalization statistics are computed using the full rollout batch before down-sampling. We conduct this comparison in the experimental setting (a) where we train Qwen2.5 (3B) on GSM8K with one L40S GPU. The results are shown in Fig. 6. We observe that computing the advantage normalization statistics using the down-sampled batch leads to better performance than using the full rollout batch. We hypothesize that the fact that the advantage normalization is consistent with the actual data used for policy updates is essential to the improved performance.

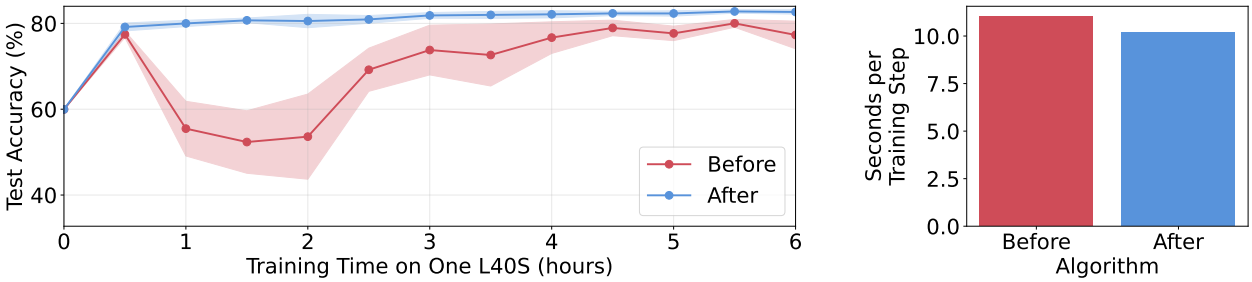

Figure 6: Performance and per-step run time comparison of the two design choices of advantage normalization in GRPO-PODS with max-variance down-sampling in experimental setting (a). "After" refers to computing the advantage normalization statistics using the down-sampled batch, while "Before" refers to doing so using the full rollout batch before down-sampling. The x-axis shows the training time, and the y-axis shows the accuracy on the test set. The shaded area represents 1.96 times the standard error of the mean.

A.4 PODS' Speed Up Ratio Over GRPO

In Fig. 3, we observe that GRPO-PODS consistently outperforms GRPO in terms of performance as the training proceeds. For each of the six plots in Fig. 3, we compute the speed up ratio of GRPO-PODS over GRPO, i.e., the ratio between the time taken by GRPO and that taken by GRPO-PODS to reach 0.99× the peak performance of GRPO. The results are shown in Table 3. We observe that our method achieves a speed up ratio between 1.7× and 3.0× over GRPO across the settings.

Table 3: Speed up ratio of GRPO-PODS over GRPO in Fig. 3.

Setting	**(a)**	**(b)**	**(c)**	**(d)**	**(e)**	**(f)**
Speed Up Ratio	2.0×	3.0×	2.0×	1.8×	1.7×	1.7×

A.5 Additional Evaluation for Experimental Settings (a) and (b)

To demonstrate that the performance improvement of GRPO-PODS over GRPO is not limited to the specific test set used in Fig. 3, we evaluate the trained models on additional test sets for experimental settings (a) and (b). For both settings, we evaluate the trained models on the GSM8K Platinum test set, which is a contamination-resistant subset of GSM8K, and MATH. The results are shown in Fig. 7. We observe that GRPO-PODS consistently outperforms GRPO across all the test sets, demonstrating the robustness of the performance improvement, and indicating the improvement is not due to overfitting to a specific test set.

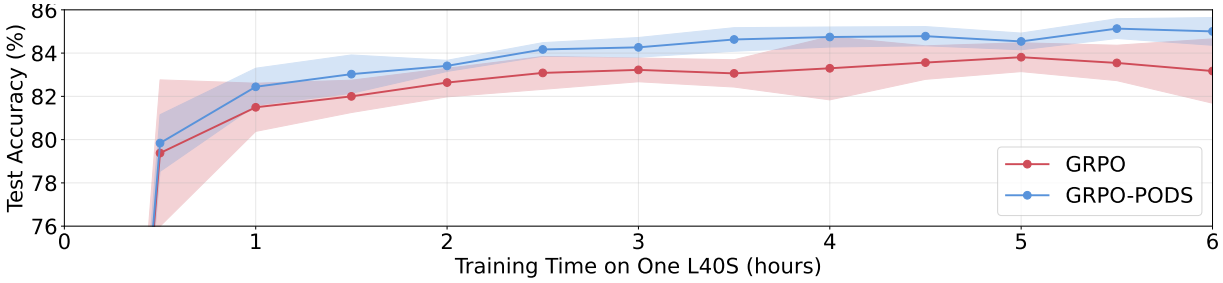

(a) Training Qwen2.5 (3B) on GSM8K with one L40S GPU and Evaluating on GSM8K Platinum

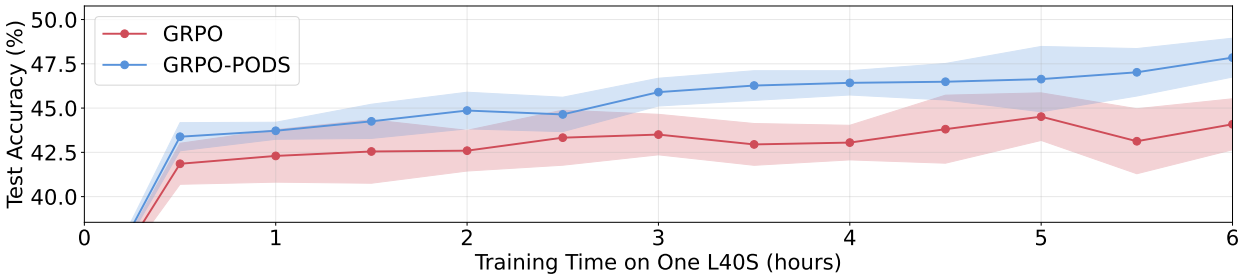

(b) Training Qwen2.5 (3B) GSM8K with one L40S GPU and Evaluating on MATH

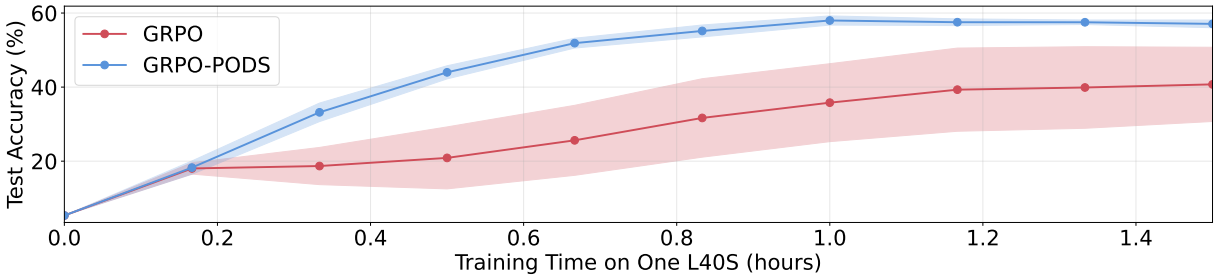

(c) Training Llama3.2 (3B) on GSM8K with one L40S GPU and Evaluating on GSM8K Platinum

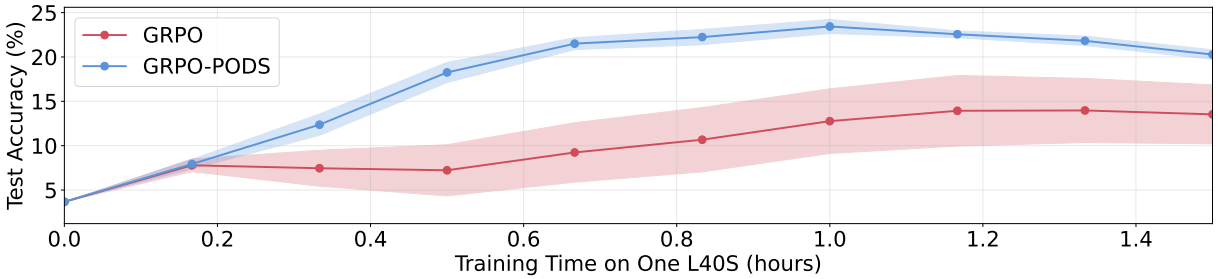

(d) Training Llama3.2 (3B) on GSM8K with one L40S GPU and Evaluating on MATH

Figure 7: Additional performance comparison of standard GRPO and GRPO-PODS with max-variance down-sampling in experimental settings (a-b). The x-axis shows the training time, and the y-axis shows the accuracy on the test set. The shaded area represents 1.96 times the standard error of the mean.

A.6 Average Completion Length Over Time

We include additional evaluation of the average completion length over the training time for each of the experiments we conduct in Section 4. We present the average completion length results in Figs. 8 to 10, in correspondence to Figs. 3 to 5 respectively. In most of the experimental settings, we observe that the average completion length stays relatively stable over the training time.

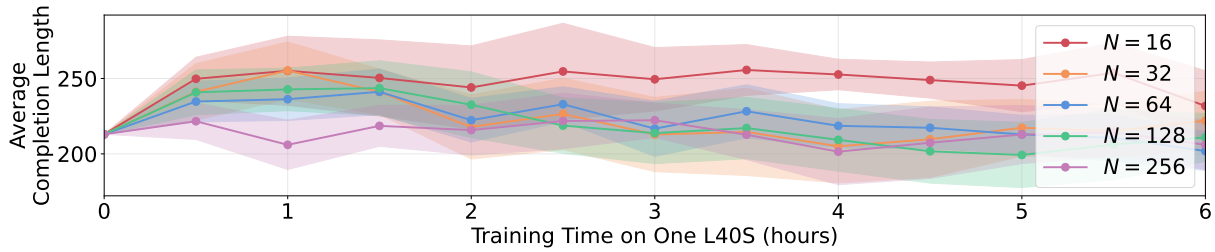

(a) Fixing $m = 16$ and varying $n \in \{16, 32, 64, 128, 256\}$

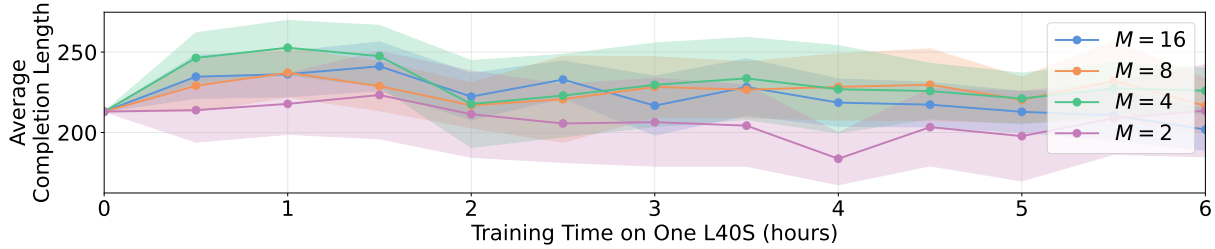

(b) Fixing $n = 64$ and varying $m \in \{16, 8, 4, 2\}$

Figure 8: Average completion length over time of the trained models in Section 4.2's experiments. The x-axis shows the training time, and the y-axis shows the average completion length in tokens. The shaded area represents 1.96 times the standard error of the mean.

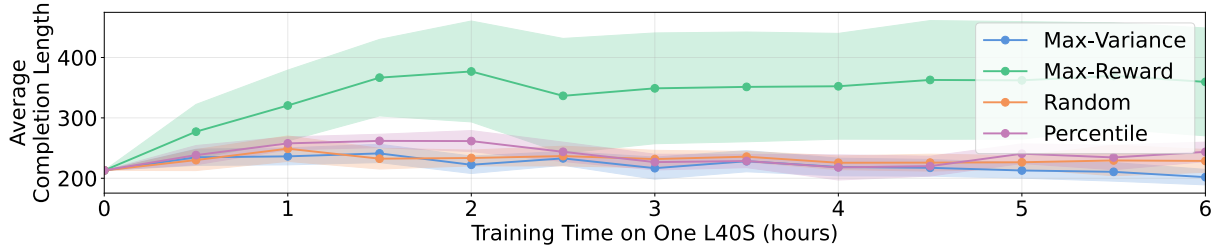

Figure 9: Average completion length over time of the trained models in Section 4.3's experiments. The x-axis shows the training time, and the y-axis shows the average completion length in tokens. The shaded area represents 1.96 times the standard error of the mean.

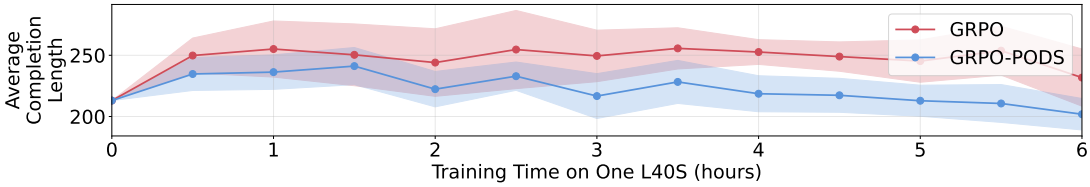

(a) Training Qwen2.5 (3B) on GSM8K with one L40S GPU

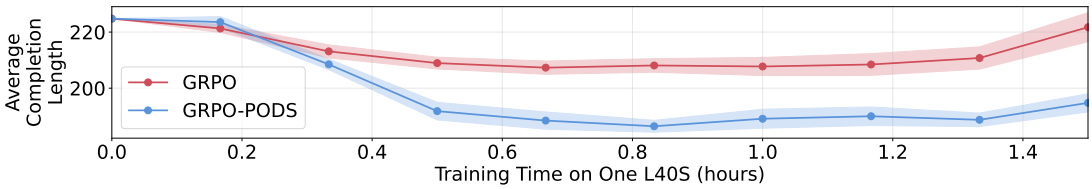

(b) Training Llama3.2 (3B) on GSM8K with one L40S GPU

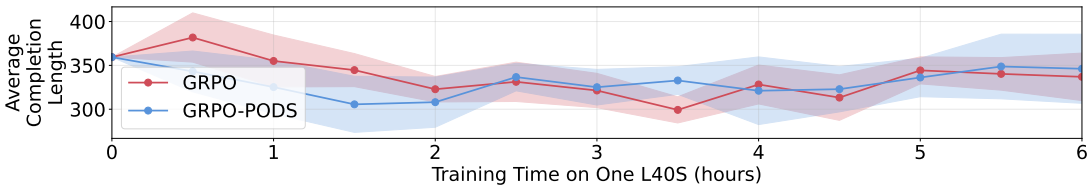

(c) Training Qwen2.5 (3B) on MATH with one L40S GPU

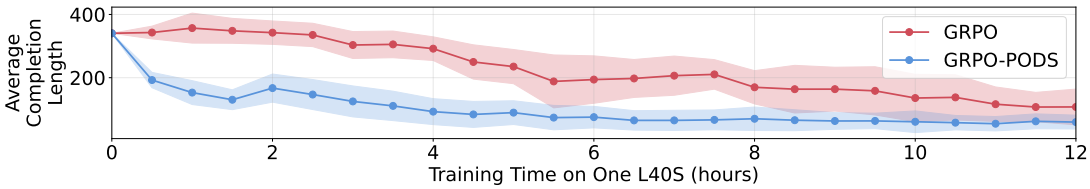

(d) Training Qwen2.5 (3B) on Chemistry with one L40S GPU

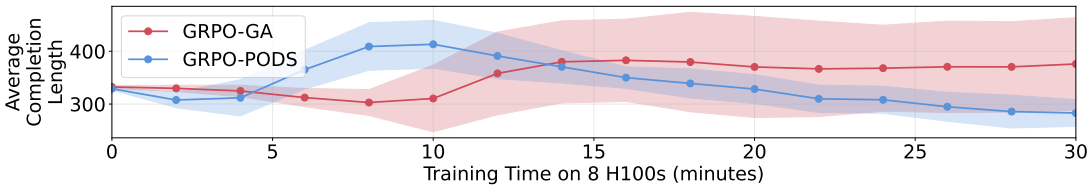

(e) Training Qwen2.5 (3B) on GSM8K with 8 H100 GPUs

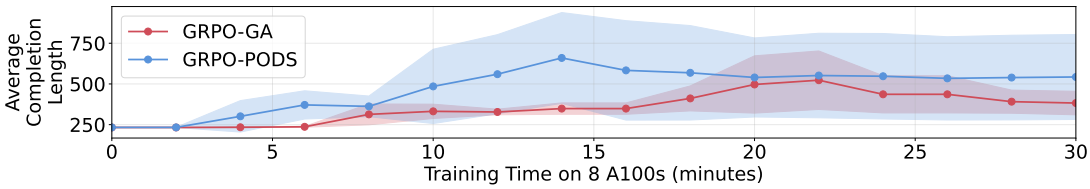

(f) Training Qwen2.5 (7B) on GSM8K with 8 A100 GPUs

Figure 10: Average completion length over time of the trained models in Section 4.1's experiments. The x-axis shows the training time, and the y-axis shows the average completion length in tokens. The shaded area represents 1.96 times the standard error of the mean.